SCIENCE WITH AN ELECTRODYNAMIC TETHER

J.R. Sanmartín

E.T.S.I. Aeronáuticos, Universidad Politécnica, Madrid, Spain

M. Hayard and M. Soudet

Alcatel Espace, Toulouse, France

ABSTRACT

Ionospheric interaction experiments using a conductive, fully bare tether are discussed. With an optimal design, requiring 1.15 mm diameter and 7.5 km full length for a collected current of 0.87 A at day conditions, the tether radiates 0.33 watts as Fast Magnetosonic waves and 0.16 watts as Alfven waves. Secondary keV electrons are produced over a 6.5 km length, giving raise to noticeable auroral effects in the D-layer, at low geomagnetic latitudes. A preliminary design of the experiment, to be implemented on either a satellite or a Station, has been carried out. An ejector gives an initial velocity to an end mass, a free spool of tether unwinding from that mass during a first stage of deployment; other phases are monitored through the tether velocity, driving a reel with an unwinding device.

Keywords: Electrodynamic Tethers, Ionospheric Experiments

1. INTRODUCTION

NETT (New Electrodynamic Tether Technology) is an experiment proposed to ESA in 1991 as part of the Columbus Precursor Flights, and originally intended to fly as exposed payload in the Shuttle cargo bay. The basic purpose was to demonstrate the capability of the innovative "bare tether" concept for electric power generation. The experiment also involves scientific experiences (artificial auroral effects, ULF and VLF wave emission) particularly suited to a bare tether.

The proposed conceptual design was recommended by a Scientific Panel of ESA, meeting in Heidelberg in March 1992. Although the Precursor Flights were finally scuttled as far as exposed payloads are concerned, the experiment is being considered in accommodation studies (APLSS, PIERS) for the European Modulus of the future International Space Station. A Phase-B engineering study has been carried out to identify critical issues, develop a deployment mechanism, and get an overall baseline design.

2. THE BARE TETHER GENERATOR

The current collected by the anodic contactor of a standard insulated tether can always be written as

$$I = J_{th} S \times G \qquad (1)$$

where $J_{th} \equiv \frac{1}{4} e n_\infty \left(\frac{8 k_B T_e}{\pi m_e} \right)^{1/2}$ is the thermal current density, S is the anodic surface area, and G is an appropriate factor; here n_∞ and T_e are the electron density and temperature in the ionosphere. Under optimal conditions n_∞ and $k_B T_e$ can reach maximum values of about $10^{12} m^{-3}$ and 0.15 eV respectively, yielding $J_{th} \simeq 0.01$ A/m^2; a current I=10 A would then require an effective collecting area $S \times G \simeq 10^3 m^2$. Actually, J_{th} may easily drop by one or even two orders of magnitude. This means that for most applications, and with realistic values of S, a large factor G (gain) will be required.

2.1 Passive spherical anode

A passive contactor that is basically characterized by a single length, in particular a sphere, as carried by TSS1, faces fundamental difficulties in attaining a large gain. For a sphere of radius R, and ignoring magnetic field effects, the anodic potential drop can be writen as

$$\phi_A \simeq \frac{k_B T_e}{e} \left(\frac{R}{\lambda_D}\right)^{4/3} \frac{G^{2/3} F(G^{1/2})}{(4\pi)^{1/3}} \simeq G^{2/3} F(G^{1/2}) \times 116 \text{ V} \qquad (2)$$

where λ_D is the ionospheric Debye length, F is a function given in Ref.1, and we finally particularised for R=0.8 m (TSS1) and maximum conditions (J_{th}=0.01 A/m^2), leading to $\lambda_D \simeq 2.9$ mm. For $S=4\pi \times (0.8 m)^2 \simeq 8 m^2$, a gain G=4 requires a bias $\phi_A \simeq 412$ V in Eq.(2) and yields I=0.32 A in Eq.(1); gains G=9, 50 require $\phi_A \simeq 1600$ V, 15.740 V and yield I≃0.72 A, 4 A, respectively. The corresponding anodic impedances would be 1.29kΩ, 2.2 kΩ and 3.9 kΩ.
Clearly, the large impedances arise from the factor $(R/\lambda_D)^{4/3}$ in Eq.(2): Since the Debye length is so short, a typical passive anode is very effectively shielded by the space-charge; it takes too large a bias ϕ_A to produce a thick sheath. Note that including magnetic guiding effects could only increase the impedance, because the electron thermal gyroradius l_e is also very small ($l_e \simeq 3.1$ cm at $k_B T_e$=0.15 eV).

2.2 Active anode

Proposed contactors circumvent these difficulties by ejecting plasma to provide quasineutrality; in addition, fluctuations due to the counterstreaming of emitted ions and attracted electrons would scatter the electrons off magnetic field lines. Ideally, the impedance should be fairly insensitive to the value of n_∞. There are, however, gross uncertainties in contactor theory; further, for the large currents of interest, it is impossible, in practice, to fully reproduce in the laboratory all dimensionless numbers, λ_D/R, l_e/R and $(SG/4\pi)^{1/2}/R$ (instead of $e\phi_A/k_B T_e$), R being some contactor "equivalent radius" (Ref.2). Flight tests are clearly needed.
PMG flight tests, reaching a maximum I≃0.3 A at $J_{th} \simeq 0.01$ A/m^2 conditions and a bias $\phi_A \simeq 130$ V, are encouraging (Ref.3). Considered as a passive contactor, a metallic box (0.3m×0.3m×0.3m) holding the PMG anode would have an equivalent radius $R \equiv \frac{1}{2} 0.3\sqrt{3}$ m ≃ 0.26 m; for ϕ_A=130 V, Eq.(2) then yields G≃5

(the lower R, the higher the gain), and Eq. (1) gives just $I \simeq 0.043$ A, or 1/7 of the measured value.
Note however that active-contactor effects amount here to increasing the effective collecting radius by just a factor $7^{1/2} \simeq 2.6$, and that the impedance $\phi_A/I \simeq 0.43$ kΩ is still high. Further, one cannot scale the results to the large currents of interest; also, measured currents showed sharp drops with n_∞, as expected from a passive contactor.

2.3 Bare tether anode

A passive anode might present a low impedance if it has two disparate characteristic lengths, as in the case of an elongated cylinder, with length $L_B \gg$ radius R. The collection is then governed by the strongest gradients, associated to R, and it will be approximately twodimensional; for $R/\lambda_D \lesssim O(1)$ and R just less than l_e, shielding and magnetic effects are negligible (OML regime), and one has $\phi_A = (k_B T_e/e)\pi G^2/4$. Further, no matter how small R, the surface $S = 2\pi R L_B$ could be large for large enough L_B.
An eastward orbiting, generator tether (current upwards), will attract electrons over some length L_B from its top, which might thus serve as cylindrical anode if left bare. Further simplicity is achieved by letting bare the entire length L_t of the tether. Ions would then be collected over a length $L_t - L_B$; since both electron current into L_B and ion current into $L_t - L_B$ are in the OML regime, and since tether bias relative to the ionosphere will vary nearly linearly with position along the tether, one has

$$\frac{I(\text{ions})}{I(\text{electrons})} \sim \left(\frac{m_e}{m_i}\right)^{1/2} \left(\frac{L_t - L_B}{L_B}\right)^{3/2}.$$

Note that too small a fraction L_B/L_t reduces both the net current I = I(electrons) - I(ions) reaching the useful load at the bottom of the tether, and the load power. For L_B/L_t too large, on the other hand, the large anodic voltage drop would reduce generator efficiency. Thus, for given values of geomagnetic field and n_∞, and a selected trade-off between generator efficiency and load power per unit mass of tether, there exists an optimal *bare-tether design*. *We find* $L_t \propto (\textit{Load power})^{1/4}$, $R_t \propto (\textit{Load power})^{3/8}$ *and* $I(\text{ions})/I(\text{electrons}) \sim L_B/L_t$ leading to $L_B/L_t \sim (m_e/m_i)^{1/5} \sim 1/7$, independently of load power (Ref. 4).
We have designed an Al bare tether for 1kW useful power and efficiency 0.75, assuming $n_\infty = 10^{12} m^{-3}$ and an electromotive force = 200 V/km. The optimal characteristics come out to be $L_t = 7.5$ km, $2R_t = 1.15$ mm, I=0.87 A (collected electron current = 0.97 A), load impedance = 1.3 kΩ. Though collecting electrons passively, the fully bare tether has a convenient property: A large drop in n_∞ from its nominal value may produce a moderate reduction in power (and efficiency), because the length L_B may adjust itself, to some extent, to the new conditions; in particular, if n_∞ drops by 1/3, the power

is found to decrease by just 20%.

3. SCIENTIFIC EXPERIENCES

The lack of insulation of our tether offers possibilities in space science not available with a standard tether.

3.1 Auroral effects

Our tether presents 6.5 km of bare metallic surface, with negative bias ranging from zero to about 1.5 kV. The ion current collected on this length is I(ions)=I−I(electrons)≃0.1 A. A typical yield of 0.1 would then give a secondary electron current of about 0.01 A, from a surface area $\pi \times 1.15$ mm $\times$ 6.5 km $\simeq$ 24 m^2. Outwardly radial acceleration of electrons within the sheath would give way, farther from the tether, to spiraling motion around the geomagnetic field , with a 2.5 m gyroradius representative of 1 keV electrons. Thus, when the tether circuit is closed, a flux of 4×10^{12} (1keV) electrons/m^2s (a fraction of $\mu A/m^2$) is injected to a field tube of 16.000 m^2 cross section in either direction.

Acceleration by the electrostatic potential of the tether being not field-aligned but roughly radial, injection takes place over a large pitch-angle range. Since this process occurs, however, at low altitudes near the Equator, the mirror ratio would be low. Most electrons would thus precipitate along field lines to the foot of the tube in the D-layer, where collisions are frequent enough to excite atoms; optical (and UV) emission from their decay should produce auroral effects. Note that fluxes of 10^{13}electrons/m^2s have been detected by low altitude polar orbiting spacecraft crossing natural auroral arcs. As our tether moves along its orbit, a pulse of magnetic disturbances and auroral lights would follow the orbital trace, at low geomagnetic latitudes; magnetometers (and not all-sky cameras) might detect it. The energy of the beam of secondary electrons could be conveniently modulated.

3.2 Wave emission

If the current along the tether is constant (or just naturally modulated by the slow changes in ambient conditions, as the tether moves along its orbit), waves are emitted in the ULF and VLF bands, corresponding to Alfven and Fast Magnetosonic branches. A recent linear analysis of impedances for an optimal bare tether gave (Ref.5)

$$Z = \frac{V_A}{c^2}\, ln\, (2e^3 L_t \Omega_i / V_S), \qquad \text{(Alfven)}$$

V_A, V_S and Ω_i being Alfven and orbital velocities and ion gyrofrequency, respectively, and

$$ZI = (m_i V_S^2 / 2\pi e^2)^{1/2} \simeq 0.38\ V, \qquad \text{(Fast Magnetosonic)}$$

this last result being actually valid for a standard tether too. For our 0.87 A current, the power radiated is 0.16 W (Alfven) and 0.33 W (Fast Magnetosonic); a fraction of mW was estimated for the TSS1 (Ref.6).

A bare tether should be quite useful in clarifying wave emission, because the strongly nonlinear region next to the tether, which must be analysed to justify linear impedance results, is described by the simplest Langmuir-probe theory (OML regime) in the bare-tether case. The nearly electrostatic field near the tether can be related to the field in the waves, which can be described in terms of an electric potential (Ref.5). There are not definite results yet on the signal reaching the ground, though a fundamental conclusion (Ref.7) is that it will involve horizontal wave vectors of order of the inverse height of the neutral atmosphere (~100 km).

4. GENERAL DESCRIPTION OF NETT

The NETT experiment can be implemented from low-orbit platforms (satellites, space stations, or last stages of launchers). We assume here that the Spacelab (for which it was originally conceived) is used. Figures 1 and 2 show general views of the device and Fig.3 gives a conceptual scheme. The total mass is about 125 kg, with an overall size of 750x700x750 mm. There are ten main subassemblies.

4.1 End mass

It weighs 30 kg and is made of *i)* a long cylinder to allow sliding on a guide; *ii)* a stationary spool of "free" tether, which unwinds through a neck under very low tension (about 0.02 N); and *iii)* a payload that includes UHF transmitter, tether tension captors, camera to measure deployment velocity, and environmental sensors.

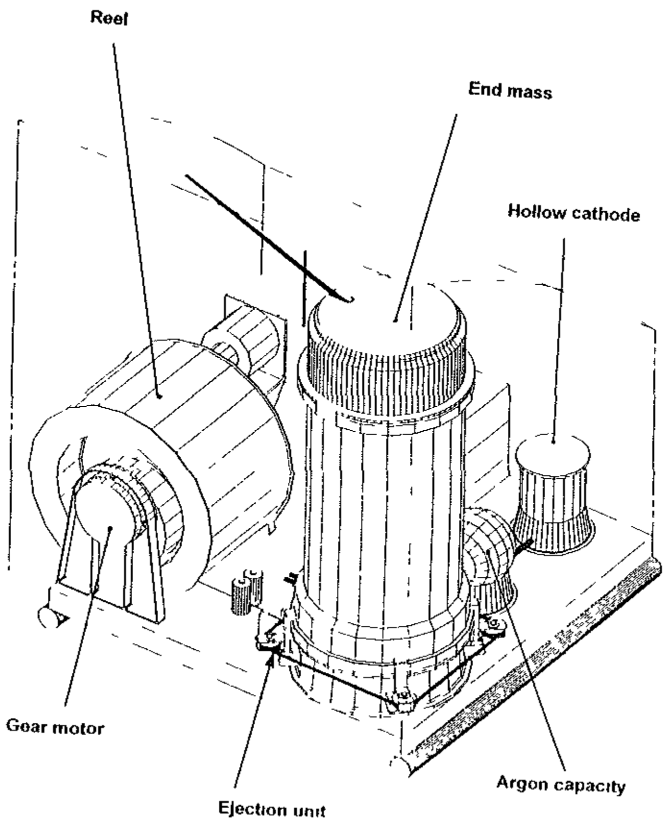

Figure 1

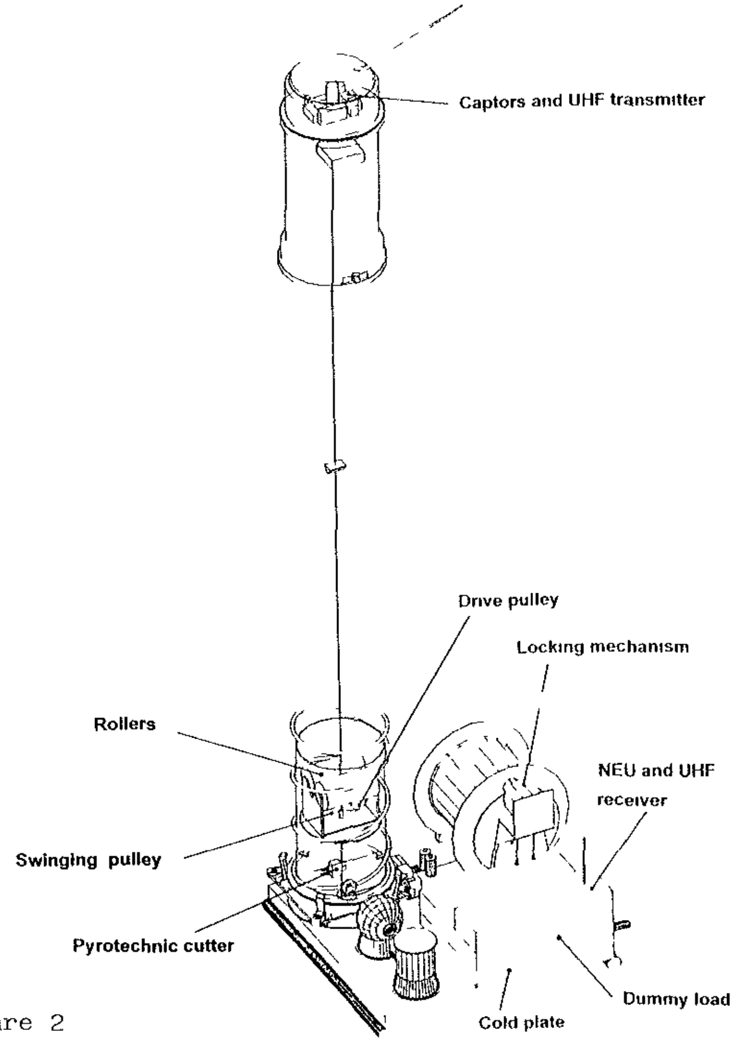

Figure 2

4 2 Tether

It is made of two parts: *i)* a thin wire of 0.5 mm diameter and 1500 m length, wound on the spool at the end mass; and *ii)* a wire of 1 15 mm diameter and 7500 m length, wound on a reel located in the platform The material is aluminum alloy, rhodium-coated to get protection against atomic axygen. The tether is marked at regular intervals to allow reading of the velocity by cameras. The 0.5 mm wire makes deployment easier at in early stage, when the gravity gradient is weak.

4.3 Ejection unit

It consists of *i)* a hollow, cylindrical core, acting as launching guide for the end mass; *ii)* a preloaded spring to provide an initial momentum at ejection; *iii)* four hooks keeping the end mass fixed in the stowed configuration; *iv)* pyrotechnic cutters to free the hooks, and *v)* a camera at the bottom of the unit, to measure the velocity of reel deployment

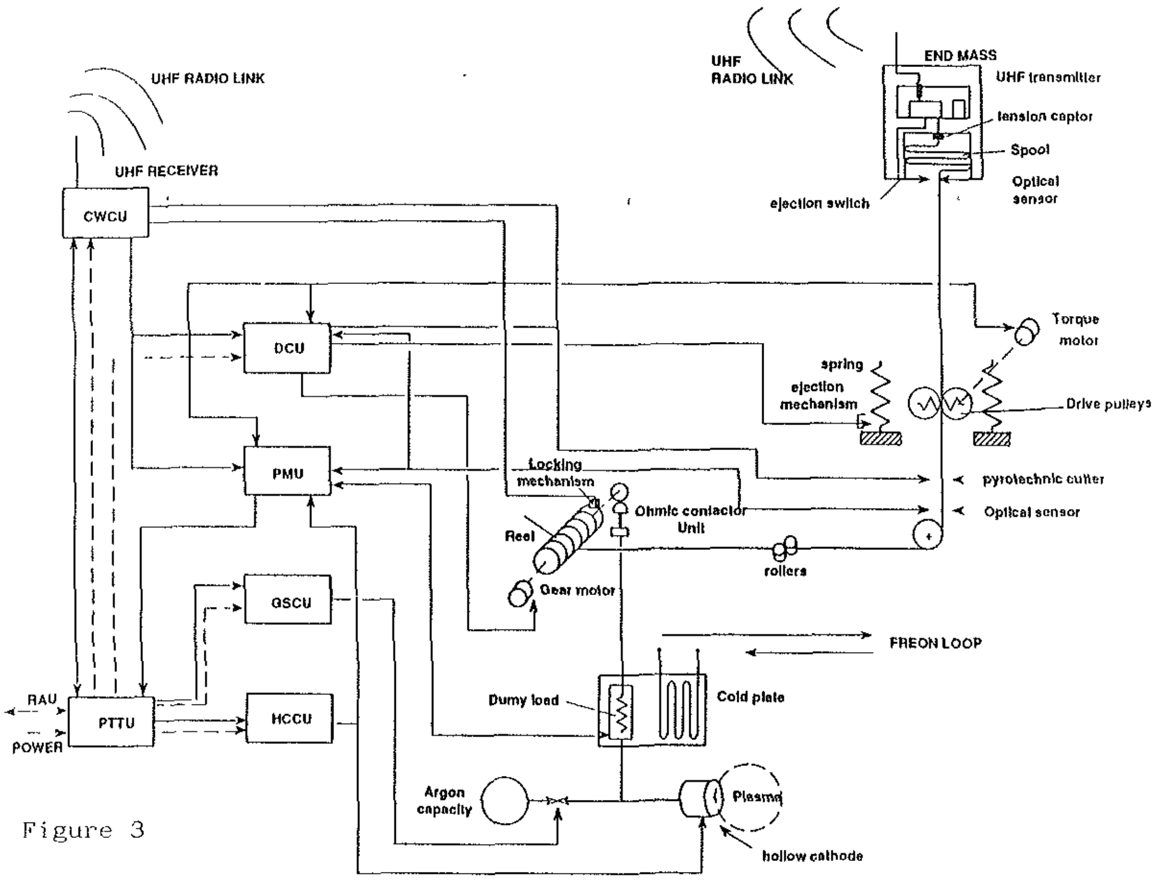

Figure 3

4.4 Reel

It is made of four parts: *i)* the reel itself, giving a predetermined velocity profile to the 1.15 mm tether, once spool unwinding at the end mass has ended; *ii)* a driving gear motor, monitoring reel motion; *iii)* a specific mechanism keeping the drumb locked during the launch phase, and once deployment is attained; and *iv)* a (graphite/copper) ohmic contactor connecting the rotating tether end to the fixed dummy load. To avoid jamming and shocks, the reel gives a controlled speed to the tether during transient phases of starting and braking, too.

4.5 Unwinder

It guides the tether along any direction above the platform through an exit neck, and holds the tether in tension to avoid jamming anywhere between reel and exit. It consists of 2 drive pulleys and 2 drive rollers mounted on ball bearings. One pulley is motorised by a torque motor that keeps the tension nearly independent of tether speed through friction (rolling without slip), which is established by the pressure of a spring on the other (swinging) pulley.

4.6 UHF link

It allows transmission of data collected at the end mass, to a receiver at platform level. Such data include tension load at the tether, and tether (or end mass) velocity, and, once integrated, deployed length of tether.

4.7 Cold plate

It is connected to the cooling freon loop provided by the mission vehicle, and to all dissipative NETT equipment (dummy load, NEU, motors).

4.8 Dummy load

It dissipates the 1 kw electric power generated by the tether. It is made of a series array of power transistors, each working at about 1A, 100 V; an aluminum plate connected to the dissipators of all individual transistors would be bolted to available points in the cold plate, providing a maximum conductance of 600 w/m^2K.

4.9 Hollow cathode

It closes the electrical circuit at platform end of the tether, with an estimated impedance of 20-30 Ω. It includes *i)* power supply for both heating and discharge, and *ii)* a spherical, thermally insulated vessel of 1 liter volume holding Argon gas at a 2×10^5 Pa initial pressure, which feeds a sonic flow to the cathode after deployment.

4.10 Nett electrical unity (NEU).

It contains units for *i)* deployment control and monitoring (DCU); *ii)* parameters measurement (PMU); *iii)* hollow cathode control (HCCU); *iv)* gas sypply control (GSCU); *v)* power, telecommand and telemetry (PTTU), and *vi)* caution and warning control (CWCU).

5. NETT IMPLEMENTATION SEQUENCE

5.1 During launch

The entire system is off:
a) The reel is locked by the locking mechanism.
b) The tether is maintained in a low tension between reel and unwinder with a mechanical clutch; this small preload, that avoids tether jamming during launch, is applied during the last integration of N.E.T.T.
c) The end mass is locked by the release mechanism located on the ejection unit.
d) UHF link, NEU, Argon capacity, hollow cathode and dummy load are off.
e) There is no freon flow in the cold plate.

5.2 *In orbit before deployment*

With the mission vehicle in orbit, dynamic solicitations are not significant but thermal effects act fully. Just before implementing deployment, we have:

a) Mission vehicle attitude is $\Phi_0=40^\circ$ ahead of radial direction.

b) NEU Freon loop circulation and system self tests (electronics, captors, dummy load, motors, hollow cathode) are put on.

5.3 Deployment

The deployment sequence starts by ejection of the end mass by a pyrotechnical order to the locking mechanism on the ejection unit. The end mass leaves the platform in the orbital plane with an angle of $\Phi_0=40^\circ$ and a radial velocity of 1.91 m/s. The tether unwinds from the spool; the UHF link and the camera in the end mass are put on by a switch. Data are recorded in the PMU and sent to the RAU (Remote Acquisition Unit).
Within a short time:
a) a few dozens of meters (programmed values defined by simulations and tests) before the end of the full unwinding in the spool (1500 m), the DCU orders to unlock the reel (acting on the reel locking mechanism);
b) the unwinder torque motor is immediately put on to maintain a tension in the tether located between reel and unwinder (about 4,5 N);
c) the reel comes in motion to give the tether the velocity and the acceleration measured at the end mass level. During this transitory phase the end mass is not stopped because the spool is not fully unwound as indicated in a). The last coils will be progressively unwound, the tension in the tether at this time being less than the gravity force acting on the end mass. Since the tension load captors are fixed at the extremity of the tether, data on tension are measured only when the spool is fully unwound. When the reel is in motion, the velocity given to the tether is measured with the platform camera insuring, via the DCU, motor gear monitoring.
The first stage ends when the tether velocity (which corresponds to the end mass radial velocity) is 2.04 m/s.
During the second stage this velocity is constant. It ends when condition $\dot{L}/L=4.1\times10^{-4}s^{-1}$ is attained. The third stage is driven under this condition until $\dot{\theta}=0$. At this time the expected value for the tether velocity is 3,8 m/s and braking begins, driving the end mass smoothly from a positive acceleration when $\dot{L}/L$ is constant, to a negative acceleration, so as to avoid a tether break or a return of the end mass. After braking the total deployed length is about 9000 m.

5.4 N.E.T.T. experiment

Once deployed, the tether is in a quasi-radial position from earth and orbiting mission vehicle, a position required to efficiently implement the NETT experiment. The following sequence is established to that end:
a) Locking the reel by action on the locking mechanism. b) Gear motor is put off. c) Argon supplies the hollow cathode by an action ordered on the valve. d) Hollow cathode power (low voltage) is put on. e) Tether is connected to the hollow cathode by an order to the dummy load. At this moment power collected in the tether is dissipated by the freon loop through the dummy load and the cold plate (about 1 kW). Plasma is generated outside the cathode. f) The experiment is monitored according to a definite schedule and specific data are recorded in both PMU and RAU (voltage, current...). The circuit is closed.

5.5 End of experiment

When the experiment is finished the following sequence is conducted:
a) The circuit is opened by an order given to the dummy load. b) The pyro-cutter acts and the tether goes away due to the gravity load acting on the end mass and due to the unwinder. c) The unwinder is then put off. d) The freon loop circulation is stopped when the temperature of the dummy load becomes acceptable. e) The NEU is put off. f) The residual parts of N.E.T.T. can support a descent (if any) in this state. The argon gas flow rate is not

stopped; it will vanish slowly.

6. REFERENCES

1. Lam S H *1965, Unified theory for the Langmuir probe in a collisionless* plasma, *Phys. Fluids, 8*, pp. 73-87.

2. Ahedo E, Martinez-Sanchez M and Sanmartin J R 1992, Current collection by an active spherical electrode in an unmagnetized plasma, *Phys. Fluids B*, 4, pp.3847-3855

3. Lilley J R 1994, Comparison of theoretical calculations with Plasma Motor Generator (PMG) experimental data, *AIAA* paper No. 94-0328.

4. Sanmartin J R, Martinez-Sanchez M and Ahedo A 1993, Bare wire anodes for electrodynamic tethers, *J. Prop. Power, 9,* pp. 353-360.

5. Sanmartin J R and Martinez-Sanchez M 1995, The radiation impedance of orbiting conductors, *J. Geophys. Res.* (to appear).

6. Donohue D J, Neubert T and Banks P M 1991, Estimating radiated power from a conducting tethered satellite system, *J. Geophys. Res.*, 96, pp. 21,245 - 21,253.

7. Estes R. 1988, Alfven Waves from an electrodynamic tethered satellite system, *J. Geophys. Res.*, 93, pp. 945-956.